

 Open access • Journal Article • DOI:10.1103/PHYSREVE.75.016106

Mean escape time in a system with stochastic volatility — Source link

Giovanni Bonanno, Davide Valenti, Bernardo Spagnolo

Institutions: University of Palermo

Published on: 23 Jan 2007 - Physical Review E (American Physical Society)

Topics: Stochastic volatility, Heston model, Geometric Brownian motion, Rendleman–Bartter model and Stochastic process

Related papers:

- [Hitting time distributions in financial markets](#)
- [Role of noise in a market model with stochastic volatility](#)
- [Volatility Effects on the Escape Time in Financial Market Models](#)
- [A Closed-Form Solution for Options with Stochastic Volatility with Applications to Bond and Currency Options](#)
- [Introduction to Econophysics: Correlations and Complexity in Finance](#)

Share this paper:    

View more about this paper here: <https://typeset.io/papers/mean-escape-time-in-a-system-with-stochastic-volatility-13ypd5gk11>

Mean escape time in a system with stochastic volatility

Giovanni Bonanno, Davide Valenti,^{*} and Bernardo Spagnolo[†]

Dipartimento di Fisica e Tecnologie Relative, Group of Interdisciplinary Physics, Università di Palermo, Viale delle Scienze, pad. 18, I-90128 Palermo, Italy

(Received 9 June 2006; revised manuscript received 29 September 2006; published 23 January 2007)

We study the mean escape time in a market model with stochastic volatility. The process followed by the volatility is the Cox, Ingersoll, and Ross process which is widely used to model stock price fluctuations. The market model can be considered as a generalization of the Heston model, where the geometric Brownian motion is replaced by a random walk in the presence of a cubic nonlinearity. We investigate the statistical properties of the escape time of the returns, from a given interval, as a function of the three parameters of the model. We find that the noise can have a stabilizing effect on the system, as long as the global noise is not too high with respect to the effective potential barrier experienced by a fictitious Brownian particle. We compare the probability density function of the return escape times of the model with those obtained from real market data. We find that they fit very well.

DOI: [10.1103/PhysRevE.75.016106](https://doi.org/10.1103/PhysRevE.75.016106)

PACS number(s): 89.65.Gh, 02.50.-r, 05.40.-a, 89.75.-k

I. INTRODUCTION

The noise in a physical system gives rise to interesting and sometimes counterintuitive effects. The stochastic resonance and the noise enhanced stability are two examples of noise activated phenomena that have been extensively studied in a wide variety of natural and physical systems such as lasers, spin systems, and chemical and biological complex systems [1–3]. Specifically the activated escape from a metastable state is important in the description of the dynamics of nonequilibrium complex systems [4,5]. Recently there has been growing interest in the application of complex system methodology to model social systems. In particular the application of statistical physics for modeling the behavior of financial markets has given rise to a new field called “econophysics” [6–9].

The stock price evolution is indeed driven by the interaction of a great number of traders. Each one follows his own strategy in order to maximize his profit. There are fundamental traders who try to invest in a solid company, speculators who try to exploit arbitrage opportunity, and noise traders who act in a nonrational way. All these considerations allow us to say that the market can be thought of as a complex system where the rationality and the arbitrariness of human decisions are modeled by using stochastic processes.

The price of financial time series was modeled as a random walk by Bachelier [10]. His model provides only a rough approximation of the real behavior of the price time series. Indeed it does not reproduce some of the stylized facts of the financial markets: (i) the distribution of relative price variation (price return) has fat tails, showing strong non-Gaussianity [7,9]; (ii) the standard deviation of the return time series, called volatility, is a stochastic process itself characterized by long memory and clustering [9,11]; (iii) autocorrelations of asset returns are often negligible [9].

A popular model proposed to characterize the stochastic nature of the volatility is the Heston model [12], where the

volatility is described by a process known as the Cox, Ingersoll, and Ross (CIR) process [13] and in mathematical statistics as the Feller process [14]. The model has been recently investigated by econophysicists [15,16] and solved analytically [17,18]. Models of financial markets reproducing the most prominent features of statistical properties of stock market fluctuations and whose dynamics is governed by nonlinear stochastic differential equations have been considered recently in the literature [19–26]. Moreover financial markets present days of normal activity and extreme days of crashes and rallies characterized by different behaviors for the volatility. The question of whether extreme days are outliers or not is still debated. This research topic has been addressed both by physicists [26] and economists [27].

A Langevin approach to the market dynamics, where market crisis was modeled through the use of a cubic potential with a metastable state, has already been proposed [8,23–25]. There feedback effects on the price fluctuations were considered in a stochastic dynamical equation for instantaneous returns. The evolution inside the metastable state represents the normal market behavior, while the escape from the metastable state represents the beginning of a crisis.

Systems with metastable states are ubiquitous in physics. Such systems have been extensively studied. In particular, it has been proven that the noise can have a stabilizing effect on these systems [2,3]. To the best of our knowledge, all of the models proposed up to now to study the escape from a metastable state contain only a constant noise intensity, which represents the volatility in econophysics. Recently theoretical and empirical investigations have been done on the mean exit time (MET) of financial time series [28,29], which is the mean time when the stochastic process leaves, for the first time, a given interval. The authors investigated the MET of asset prices outside a given interval of size L , and they found that the MET follow a quadratic growth in terms of the region size L . Their theoretical investigation was done within the formalism of the continuous time random walk. Within the same formalism the statistical properties of the waiting times for high-frequency financial data have been investigated in Ref. [30].

^{*}Email address: valentid@gip.dft.unipa.it

[†]Email address: spagnolo@unipa.it

In this work we model the volatility with the CIR process and investigate the statistical properties of the escape times when both an effective potential with a metastable state and the CIR stochastic volatility are present. Our study provides a natural evolution of the models with constant volatility. The analysis has the purpose to investigate the role of the noise in financial market extending a popular market model and to provide a starting model for physical systems under the influence of a fluctuating noise intensity. The paper is organized as follows. In the next section the modified Heston model and the noise enhanced stability effect are described. In the third section the results for two extreme cases of this model are reported. In Sec. IV we comment on the results for the general case and the probability density function of the escape time of the returns, obtained by our model, is compared with that extracted from experimental data of a real market. In the final section we draw our conclusions.

II. THE MODIFIED HESTON MODEL AND THE NES EFFECT

The Heston model, which describes the dynamics of stock prices $p(t)$ as a geometric Brownian motion with the volatility given by the CIR mean-reverting process, is defined by the following Ito stochastic differential equations:

$$dp(t) = \mu p dt + \sigma(t) p dW_1(t), \quad (1)$$

$$dv(t) = a[b - v(t)]dt + c\sqrt{v(t)}dW_2(t), \quad (2)$$

where $\sigma(t)$ is the time-dependent volatility, $v(t) = \sigma^2(t)$ and $W_i(t)$ are uncorrelated Wiener processes with the usual statistical properties

$$\langle dW_i \rangle = 0, \quad \langle dW_i(t) dW_j(t') \rangle = dt \delta(t - t') \delta_{i,j}. \quad (3)$$

In Eq. (1) μ represents a drift at macroeconomic scales. In Eq. (2) the square of the volatility reverts towards a macroeconomic long time term given by the mean value b , with a relaxation time a^{-1} . Here c is the amplitude of volatility fluctuations often called the volatility of volatility. By introducing log returns $x(t) = \ln[p(t)/p(0)]$ in a time window $[0, t]$ and using Ito's formula [31], we obtain the stochastic differential equation (SDE) for $x(t)$

$$dx(t) = [\mu - v(t)/2]dt + \sqrt{v(t)}dW_1(t). \quad (4)$$

Here we consider a generalization of the Heston model, by replacing the geometric Brownian motion with a random walk in the presence of a cubic nonlinearity. This generalization represents a fictitious ‘‘Brownian particle’’ moving in an effective potential with a metastable state, in order to model those systems with two different dynamical regimes similar to financial markets in normal activity and extreme days [23–25]. The equations of the new model are

$$dx(t) = -\left(\frac{\partial U}{\partial x} + \frac{v(t)}{2}\right)dt + \sqrt{v(t)}dW_1(t), \quad (5)$$

$$dv(t) = a(b - v(t))dt + c\sqrt{v(t)}dW_2(t), \quad (6)$$

where $U(x) = Ax^3 + Bx^2$ is the effective cubic potential shown in Fig. 1 with $A=2$ and $B=3$. From now on we call the first

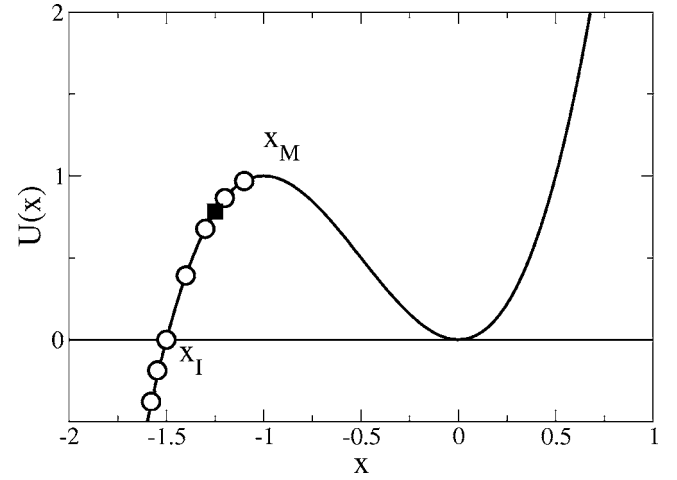


FIG. 1. Cubic potential used in the dynamical equation for the variable $x(t)$. The points evidenced in the figure indicate the starting positions x_0 used for the simulations illustrated in Sec. III (white circles) and Sec. IV (black square).

and second term of Eq. (6) reverting term and noise term, respectively.

Let us call x_M the abscissa of the potential maximum and x_I the cross point between the potential and the x axes. The intervals $x_0 < x_I$ and $I = [x_I, x_M]$ are clearly regions of instability for the system. In systems with a metastable state, the random fluctuations can originate the noise enhanced stability (NES) phenomenon, an interesting effect that increases the stability, enhancing the lifetime of the metastable state [2,3]. The mean escape time τ for a Brownian particle moving throughout a barrier ΔU is given by the well known exponential Kramers law [31,32]

$$\tau = C \exp\left[\frac{\Delta U}{v}\right], \quad (7)$$

where τ is a monotonically decreasing function of the noise intensity v , and C is a prefactor which depends on the potential profile. This is true only if the random walk starts from initial positions inside the potential well. When the starting position is chosen in the instability region $x_0 < x_M$, τ exhibits an enhancement behavior, with respect to the deterministic escape time, as a function of v . This is the NES effect and it can be explained by considering the barrier ‘‘seen’’ by the Brownian particle starting at the initial position x_0 , that is $\Delta U_{in} = U(x_{max}) - U(x_0)$. Moreover ΔU_{in} is less than ΔU as long as the starting position x_0 lies in the interval $I = [x_I, x_M]$. Therefore for a Brownian particle starting from an unstable initial position it is more likely to enter into the well than to escape from, once the particle has entered. So a small amount of noise can increase the lifetime of the metastable state. For a detailed discussion on this point and different dynamical regimes see Refs. [3]. For increasing noise intensities, the Kramers behavior is recovered.

We have already investigated the statistical properties of the escape times for models with stochastic volatility, namely, the Heston model and the GARCH model [16]. We found that the probability density function of the escape

times obtained in the Heston model exhibits a better agreement with real data than that calculated in the GARCH model. Here, by considering the modified Heston model [Eqs. (5) and (6)], characterized by a stochastic volatility and a nonlinear Langevin equation for the returns, we study the mean escape time as a function of the model parameters a , b , and c . In particular we investigate whether it is possible to observe some kind of nonmonotonic behavior such as that observed for τ vs v in the NES effect with constant volatility v . We find a nonmonotonic behavior of the mean escape time (MET) τ , as a function of the model parameters. Within this behavior we recognize the enhancement of τ as a NES effect in a broad sense.

Our modified Heston model has two limit regimes, corresponding to the cases $a=0$, with only the noise term in the equation for the volatility $v(t)$, and $c=0$ with only the reverting term in the same equation. This last case corresponds to the usual parametric constant volatility regime. In fact, apart from an exponential transient, the volatility reaches the asymptotic value b . The NES effect should be observable in the latter case as a function of b , which is the average volatility. In fact, in this case we recover the motion of a Brownian particle in a fixed cubic potential with a metastable state and an enhancement of its lifetime for particular initial conditions.

For this purpose we perform simulations by numerically integrating Eqs. (5) and (6) using a time step $\Delta t=0.01$ and, as potential parameters, $A=2$ and $B=3$. All the integration steps yielding negative values for v were rejected and repeated. The simulations were performed placing the walker in the initial positions x_0 located in the unstable region $[x_I, x_M]$ (see Fig. 1) and using an absorbing barrier at $x=-6.0$. Each time the walker hits the barrier, the escape time is registered and another simulation starts, placing the walker at the same initial position x_0 , but using the volatility value of the barrier hitting time.

III. LIMIT CASES

First of all we present the result obtained in the limit cases where we have only one of the two terms in the CIR equation (6). Namely, (a) only the reverting term ($a \neq 0, b \neq 0, c = 0$, revert-only case), and (b) only the noise term ($a=0, b$ whatever, $c \neq 0$, noise-only case) are present. In the case (a) the volatility is practically constant and equal to b , apart from an exponential transient that is negligible for times $t \gg a^{-1}$.

The mean escape time as a function of b is plotted in Fig. 2(a) for the seven different initial positions indicated in Fig. 1 (white circles in that figure). The curves are averaged over 10^5 escape events. The nonmonotonic behavior is present. The escape time increases by increasing b until it reaches a maximum. After the maximum, when the values of b are much greater than the potential barrier height, the Kramers behavior is recovered. The nonmonotonic behavior is more evident for starting positions near the maximum of the potential. For starting positions x_0 lying in the interval $I = [x_I, x_M]$, the initial plateau is an artifact of the calculus. Indeed in the theoretical solution for the constant volatility

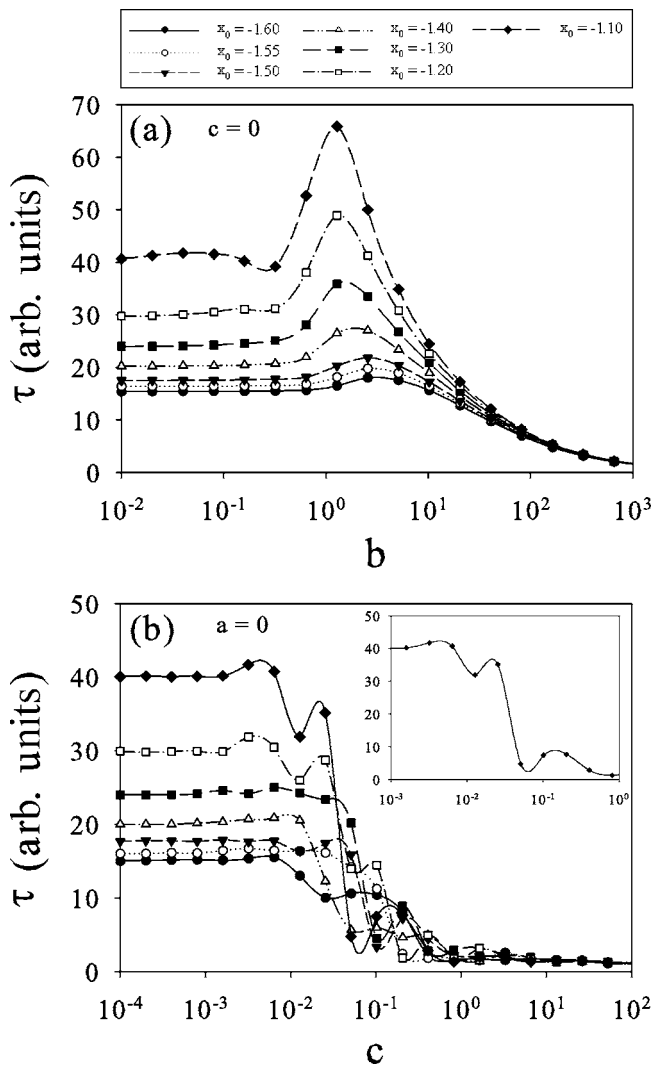


FIG. 2. Mean escape time τ for the seven different starting positions of Fig. 1 (white circles in that figure). Limit cases where only one of the two terms in the CIR equation is present: (a) τ vs b , when only the reverting term is present ($a=10^{-2}, c=0$), and (b) τ vs c , when only the noise term is present ($a=0, b=10^{-2}$). The different starting positions x_0 from top to bottom are $-1.1, -1.2, -1.3, -1.4, -1.5, -1.55, -1.60$. The parameters b and c are dimensionless, while a , measured in arbitrary units, has dimension of the inverse time. Inset: detail of the curve with $x_0=-1.10$.

case, τ diverges as the noise intensity approaches zero [2,3]. With such a noise intensity the escape from the well is a very unlikely event. We should require an extremely great number of simulation steps in order to observe an event pushing the particle into the well.

In case (b), v is a multiplicative stochastic process with standard deviation equal to c . The random term in Eq. (6) is given by the product of the white noise and the square root of the process itself v . In Fig. 2(b) we plot τ as a function of the parameter c . The nonmonotonic behavior is absent and the MET decreases monotonically, but differently from the Kramers behavior. The curves are averaged over 10^8 escape events. In this case a greater number of events is required to eliminate the fluctuations present in the curves. Once again

we cannot draw any conclusions for the constant behavior of τ , when the values of the parameter c are very small, because of the finite number of simulation steps [3]. It is worthwhile pointing out that the NES effect is not observable as a function of the parameter c , if $a=0$. Therefore, the presence of the reverting term affects the behavior of τ in the domain of the noise term of the volatility and it regulates the transition from nonmonotonic to monotonic regimes of MET. Moreover in this noise-only regime the volatility is proportional to the square of the Wiener process and therefore the fluctuations during the monotonic decreasing behavior of τ are very large. We see three different dynamical regimes: (i) for low values of the parameter c , with respect to the height of the potential barrier, we have a constant behavior, (ii) for intermediate values of c we have fluctuations with decreasing monotonic behavior, (iii) for values of c greater than 1, which is exactly the height of the barrier, we get very small and constant values of τ close to zero. This behavior is mainly due to the presence of the Ito term in Eq. (5) for the log returns $x(t)$. In fact, because of this term we have a fluctuating potential, obtained by the previous one by adding a linear term $U' = U(x) + (xv)/2$. The effect of the positive linear term is to modify randomly the potential shape in such a way that the potential barrier disappears for greater values of the volatility $v(t)$. Specifically for values of $v < 3$ the potential barrier is always present, while for $v > 3$ it disappears. This produces a random enhancement of the escape process with a consequent decreasing behavior of the average escape time.

IV. GENERIC CASE

In order to present our results for the generic case, where both the reverting and noise terms of the CIR equation are present, we focus on a single starting position $x_0 = -1.25$, which is located in the middle of the interval $[x_I, x_M]$. We analyze the escape time through the barrier using different values for parameters a , b , and c . We note that the average escape time τ is measured in arbitrary units (a.u.), the parameter a (measured in a.u. too) has the dimension of the inverse time, while b and c are dimensionless.

As a first result we present the behavior observed for τ as a function of the reverting level b . In Fig. 3 we show the curves averaged over 10^5 escape events. Each panel corresponds to a different value of c . Inside each panel different curves correspond to different values of a spanning seven orders of magnitude. The nonmonotonic shape, characteristic of the NES effect, is clearly shown in Fig. 3(a). This behavior is shifted towards higher values of b as the parameter a decreases, and it is always present. In Fig. 3(c), which corresponds to a much greater value of c ($c=30$), all the curves are monotonic but with a large plateau. So an increase in the value of c causes the NES effect to disappear.

To understand this behavior let us note that the parameters a and c play a regulatory role in Eq. (4). For $a \gg c$ the drift term is predominant while for $a \ll c$ the dynamics is driven by the noise term, unless the parameter b takes great values. In fact in Fig. 3(a) the nonmonotonic behavior is observed for $a \ll c$, provided that $b \gg c$. For increasing values of a the

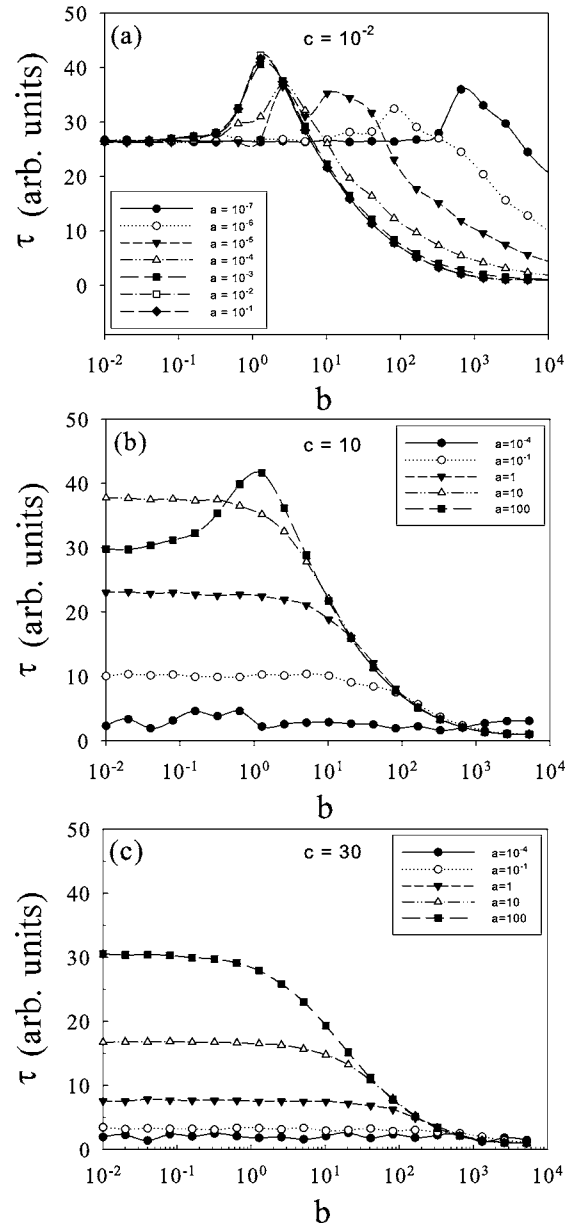


FIG. 3. Mean escape time τ as a function of the reverting level b . Each panel corresponds to a different value of c , specifically (a) $c=10^{-2}$, (b) $c=10$, and (c) $c=30$. Inside each panel different curves correspond to the following values of a : (a) black circle 10^{-7} , white circle 10^{-6} , black triangle down 10^{-5} , white triangle up 10^{-4} , black square 10^{-3} , white square 10^{-2} , black diamond 10^{-1} ; (b) and (c) black circle 10^{-4} , white circle 10^{-1} , black triangle down 1, white triangle up 10, black square 10^2 .

system approaches the revert-only regime and we recover the behavior shown in Fig. 2(a). For $a \ll c$ the shape of the curves changes. The mean escape time τ is almost constant, and only for very high values of b we observe a decreasing behavior. This happens because, for smaller values of a the reverting term becomes negligible in comparison with the noise term and the dependence on b becomes weaker. Only when b is large enough the reverting term assumes values that are no more negligible with respect to the noise term and we can observe again a dependence of τ on b . By increasing

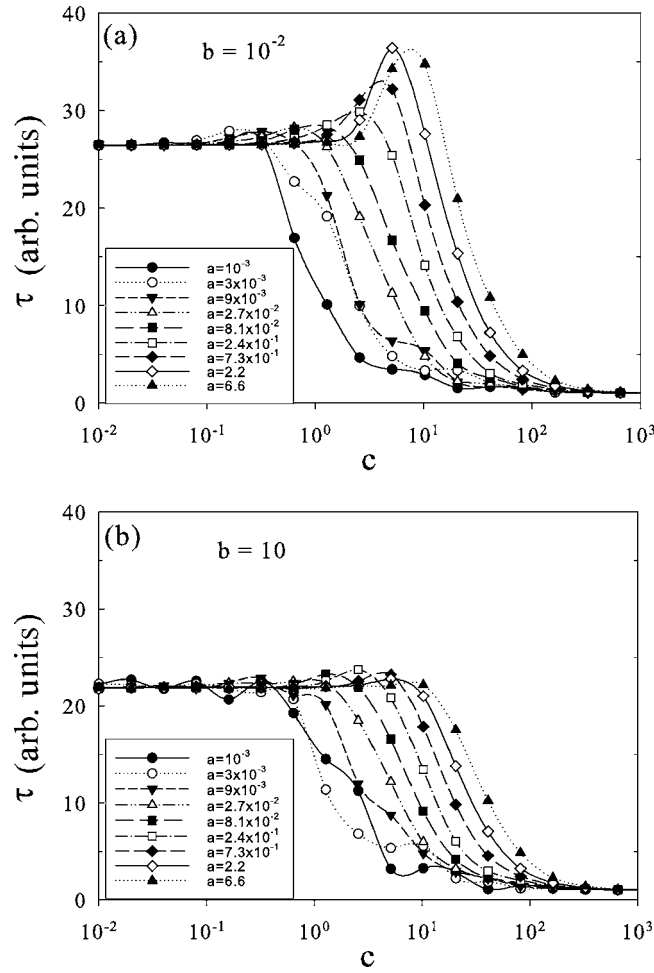


FIG. 4. Mean escape time τ as a function of the noise intensity c . Each panel corresponds to a different value of b , specifically (a) $b=10^{-2}$ and (b) $b=10$. Inside each panel different curves correspond to the following values of a : black circle 10^{-3} , white circle 3×10^{-3} , black triangle down 9×10^{-3} , white triangle up 2.7×10^{-2} , black square 8.1×10^{-2} , white square 2.4×10^{-1} , black diamond 7.3×10^{-1} , white diamond 2.2, black triangle up 6.6.

the value of c we observe the nonmonotonic behavior only for a very great value of the parameter a , that is for $a=100 \gg c$ [see Fig. 3(b)]. For further increase of parameter c [see Fig. 3(c)], the noise experienced by the system is much greater than the effective potential barrier “seen” by the fictitious Brownian particle and the NES effect is never observable. Moreover we are near a noise-only regime, and we can say that the magnitude of c is so high as to saturate the system.

In summary the NES effect can be observed as a function of the volatility reverting level b , the effect being modulated by the parameter $(ab)/c$. The phenomenon disappears if the noise term is predominant in comparison with the reverting term. Moreover the effect is no more observable if the parameter c pushes the system towards a too noisy region.

As a second step we study the dependence of τ on the noise intensity c . Figure 4 shows the curves of τ vs c , averaged over 10^5 escape events. Each panel corresponds to a different value of b . Inside each panel different curves cor-

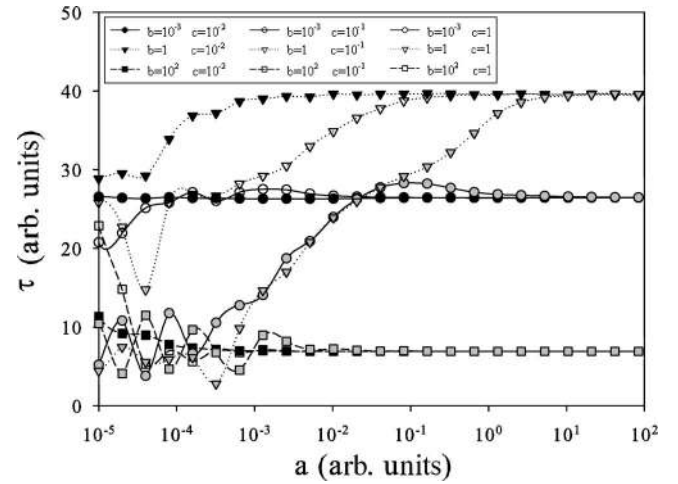


FIG. 5. Mean escape time τ as a function of the reverting rate a for different values of b and c . Curves with the same color correspond to the same value of c , while curves with the same symbol correspond to the same value of b . Specifically the values of b used are 10^{-3} circle, 1 triangle, 10^2 square. The values of c used are 10^{-2} black, 10^{-1} white, 1 gray.

respond to different values of a . The shape of the curves is similar to that observed in Fig. 3. For small b [panel (a)] we observe a nonmonotonic behavior, while for great b [panel (b)] the curves are monotonic but with a large plateau. Let us recall the results of Fig. 2(b): there was no NES effect in the noise-only case. So for small values of a , when the reverting term is negligible, the absence of the nonmonotonic behavior is expected. By increasing a the nonmonotonic behavior is recovered [see Fig. 4(a)]. Once again, if one of the parameters pushes the system into a high noise region, the nonmonotonic behavior disappears [see Fig. 4(b)]. Specifically if b is high, the reverting term drives the system towards values of volatility that are outside the region where the NES effect is observable. Indeed a direct inspection of Fig. 3 shows that the value of b used in Fig. 4(b) is located after the maximum of τ for all values of a and c .

In summary when the noise term is coupled to the reverting term we observe the NES effect on the variable c . The effect disappears if b is so high as to saturate the system. As a last result we discuss the behavior observed for τ as a function of the reverting rate a . This allows us to observe the transition between the two regimes of the process discussed above: the noise-only regime and the revert-only regime. The results are reported in Fig. 5 for three different values of b and three different values of c . To reduce the fluctuations in all the curves when the parameter a becomes small, we performed simulations by averaging on 10^6 escape events. It is worthwhile to note that for values of the parameter $a < 10^{-5}$, we enter into the noise-only regime, which characterizes one of the limit cases discussed in Sec. III. Curves with the same color correspond to the same value of c while curves with the same symbol correspond to the same value of b .

The system tends to the noise-only regime for lower values of a and to the revert-only regime for higher values of a . On the right end of Fig. 5 the curves corresponding to the

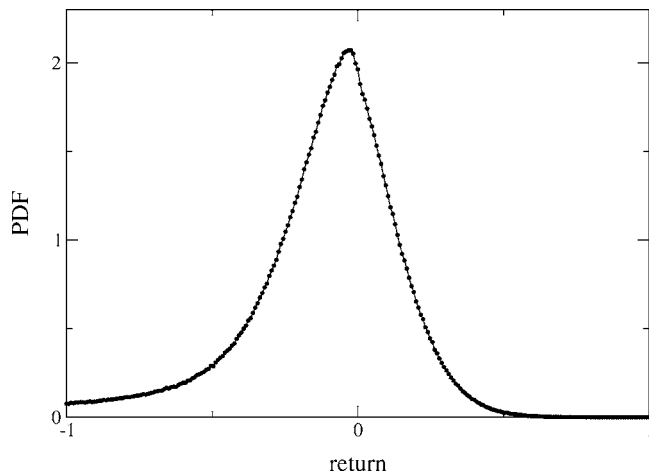


FIG. 6. Probability density function of the stock price returns for our model [Eqs. (5) and (6)]. The values of the parameters are $a = 10^{-1}$, $b=4.5$, and $c=2 \times 10^{-1}$. The potential parameters are $A=2$ and $B=3$.

same value of b tend to group together. The values of τ the curves approach reflect the nonmonotonic behavior observed in Fig. 3(a). Indeed all the curves corresponding to the intermediate value of b ($b=1$) approach a value of τ , which almost corresponds to the maximum value of MET in Fig. 3(a) [we note that the behavior for $a=10^{-1}$ coincides with that for $a=1$, even if it is not reported in Fig. 3(a)]. This value of τ is greater than that reached by the curves corresponding to other two, lower and greater, values of b (10^{-3} and 10^2 , respectively). Conversely on the left end the curves corresponding to the same value of c tend to group together. It is worth noting that in this last case the curves with the highest value of c , namely, $c=1$, show greater fluctuations as those observed in all the previous cases where the noise term is predominant [see, for example, Fig. 2(b)].

It is interesting to show, for our model [Eqs. (5) and (6)], some of the well-established statistical signatures of the financial time series, such as the probability density function (PDF) of the stock price returns, the PDF of the volatility, and the return correlation. In Fig. 6 we show the PDF of the returns. To quantitatively characterize this PDF with regard to the width, asymmetry, and fatness of the distribution, we calculate the mean value $\langle \Delta x \rangle$, the variance $\sigma_{\Delta x}$, the skewness κ_3 , and the kurtosis κ_4 . We obtain the following values: $\langle \Delta x \rangle = -0.162$, $\sigma_{\Delta x} = 0.348$, $\kappa_3 = -1.958$, and $\kappa_4 = 5.374$. These statistical quantities clearly show the asymmetry of the distribution and its leptokurtic nature observed in real market data. In fact, the empirical PDF is characterized by a narrow and large maximum, and fat tails in comparison with the Gaussian distribution [7,8]. Specifically we note that the value of the kurtosis $\kappa_4 = 5.374$, which gives a measure of the distance between our distribution and a Gaussian one, is of the same order of magnitude as that obtained for the S&P 500 for daily prices (see Fig. 7.2 on page 114 of Ref. [8]). The presence of the asymmetry is very interesting and is the subject of future investigations. This asymmetry is due to the nonlinearity introduced in the model through the cubic potential (see Fig. 1). Of course, a comparison between the

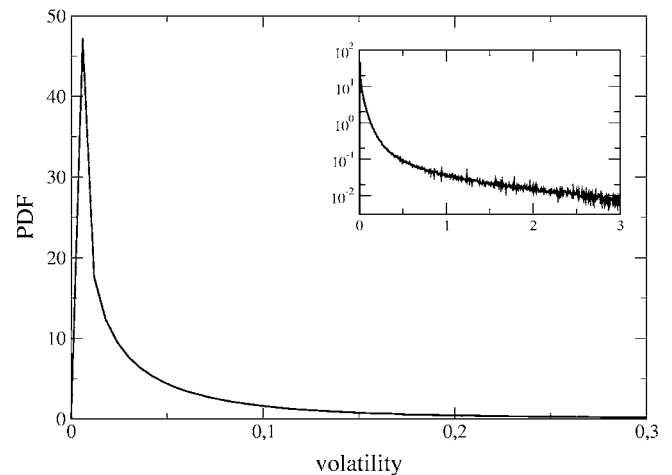


FIG. 7. Probability density function of the volatility for our model [Eqs. (5) and (6)]. The values of the parameters are the same as in Fig. 6. Inset: semilog plot of the PDF of volatility in a longer time scale.

PDF of real data and that obtained from the model requires further investigations on the dynamical behavior of the system, as a function of the model parameters. In Fig. 7 we show the PDF of the volatility for our model, and we can see a log-normal behavior as that observed approximately in real market data. Finally, in Fig. 8 we show the correlation function of the returns. As we can see, the autocorrelations of the asset returns are insignificant except for the very small time scale for which microstructure effects come into play. This is in agreement with one of the stylized empirical facts emerging from the statistical analysis of price variations in various types of financial markets [9]. A quantitative agreement of the PDF of volatility and the correlation of returns with the corresponding quantities obtained from real market data is the subject of further studies.

Our last investigation concerns the PDF of the escape time of the returns, which is the main focus of our paper. By using our model [Eqs. (5) and (6)], we calculate the probability density function for the escape time of the returns. We

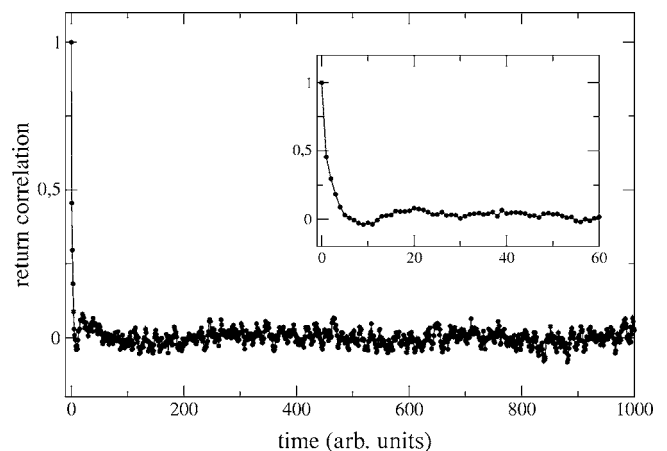


FIG. 8. Correlation function of the returns for our model [Eqs. (5) and (6)]. The values of the parameters are the same as in Fig. 6. Inset: detail of the behavior at short times.

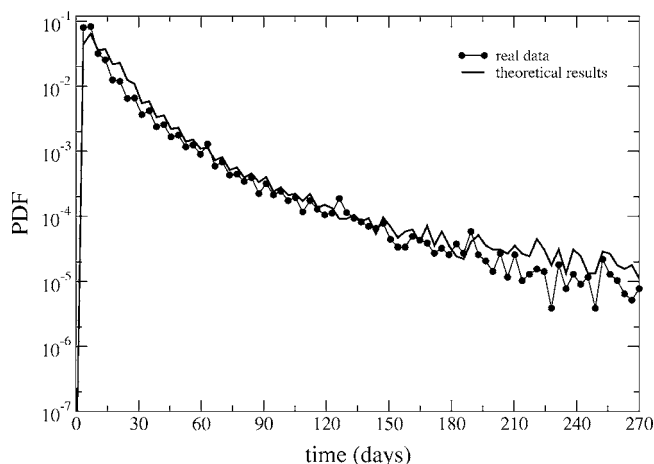


FIG. 9. Probability density function of the escape time of the returns from simulation (solid line), and from real data (black circle). The values of the parameters are $\Delta x_i = -0.1\sigma_{\Delta x}$, $\Delta x_f = -1.0\sigma_{\Delta x}$, $x_0 = -1.25$, $x_{\text{abs}} = -6.0$, $v_{\text{start}} = 8.62 \times 10^{-5}$, $a = 10^{-1}$, $b = 4.5$, and $c = 2 \times 10^{-1}$. The potential parameters are $A = 2$ and $B = 3$.

define two thresholds Δx_i and Δx_f , which represent the start point and the end point for calculating τ , respectively. When the return series reaches the value Δx_i , the simulation starts to count the time τ and it stops when the threshold Δx_f is crossed. In order to fix the values of the two thresholds we consider the standard deviation (SD) $\sigma_{\Delta x}$ of the return series over a long time period corresponding to that of the real data. Specifically $\sigma_{\Delta x}$ is the average of the standard deviations σ_n observed for each stock during the above mentioned whole time period (n is the stock index, varying between 1 and 1071). Then we set $\Delta x_i = -0.1 \sigma_{\Delta x}$ and $\Delta x_f = -1.0 \sigma_{\Delta x}$. We perform our simulations obtaining a number of time series of the returns equal to the number of stocks considered, which is 1071. The initial position is $x_0 = -1.25$ and the absorbing barrier is at $x_{\text{abs}} = -6.0$. For the CIR stochastic process v , we choose $v_{\text{start}} = 8.62 \times 10^{-5}$, $a = 10^{-1}$, $b = 4.5$, and $c = 2 \times 10^{-1}$. The choice of this parameter data set is not based on a fitting procedure as that used for example in Ref. [18]. There the minimization of the mean square deviation between the PDF of the returns, extracted from financial data, and that obtained theoretically is done. We choose the parameter set in the range in which we observe the nonmonotonic behavior of the mean escape time of the price returns as a function of the parameters b and c . Then by a trial and error procedure we select the values of the parameters a , b , and c for which we obtain the best fitting between the PDF of the escape times calculated from the modified Heston model [Eqs. (5) and (6)] and that obtained from the time series of real market data. We report the results in Fig. 9. Of course a better quantitative fitting procedure could be done, by considering also the potential parameters. This detailed analysis will be done in a forthcoming paper.

As real data we use the daily closure prices for 1071 stocks traded at the NYSE and continuously present in the 12-year period 1987–1998 (3030 trading days). The same data set was used in previous investigations [16,17,33,34]. From this data set we obtain the time series of the returns and we calculate the time to hit a fixed threshold starting from a fixed initial position. The two thresholds were chosen as a fraction of the average standard deviation $\sigma_{\Delta x}$ on the whole time period, as we have done in simulations. The agreement between real data and those obtained from our model is very good. We note that at high escape times the statistical accuracy is worse because of few data with high values. The parameter values of the CIR process for which we obtain good agreement between real and theoretical data are in the range in which we observe the nonmonotonic behavior of MET [see Fig. 3(a)]. This means that in this parameter region we observe a stabilizing effect of the noise on the prices in the time windows for which we have a variation of returns between the two fixed values Δx_i and Δx_f . This encourages us to extend our analysis to large amounts of financial data and to explore other parameter regions of the model.

V. CONCLUSIONS

We studied the mean escape time in a market model with a cubic nonlinearity coupled with a stochastic volatility described by the Cox-Ingersoll-Ross equation. In the CIR process the volatility has fluctuations of intensity c and it reverts to a mean level b at rate a .

Our results show that as long as the mean level a is different from zero it is possible to observe a nonmonotonic behavior of MET as a function of the two model parameters b and c . The parameter a regulates the transition from a noise-only regime, where the reverting term is absent or negligible, to a revert-only regime, where the noise term is absent or negligible. In the former case, the enhancement of MET with a nonmonotonic behavior as a function of the model parameters, that is the NES effect, is not observable. The curves have a monotonic shape with a plateau. Moreover, if one of the parameters is so big to push the system into a region where the noise is greater than the barrier height of the effective potential, the effect is no more observable at all. In the revert-only regime, instead, the NES phenomenon is recovered. With its regulatory effect, the reverting rate a can be used to modulate the intensity of the stabilizing effect of the noise observed by varying b and c . In this parameter region the probability density function of the escape times of the returns fits very well that obtained from the experimental data extracted by the real market.

ACKNOWLEDGMENTS

The authors wish to thank Dr. F. Lillo for useful discussions. This work was supported by MIUR, INFN-CNR, and CNISM.

- [1] L. Gammaitoni, P. Hänggi, P. Jung, and F. Marchesoni, *Rev. Mod. Phys.* **70**, 223 (1998); V. S. Anishchenko, A. B. Neiman, F. Moss, and L. Schimansky-Geier, *Phys. Usp.* **42**, 7 (1999); R. N. Mantegna, B. Spagnolo, and M. Trapanese, *Phys. Rev. E* **63**, 011101 (2001); T. Wellens, V. Shatokhin, and A. Buchleitner, *Rep. Prog. Phys.* **67**, 45 (2004).
- [2] R. N. Mantegna and B. Spagnolo, *Phys. Rev. Lett.* **76**, 563 (1996); D. Dan, M. C. Mahato, and A. M. Jayannavar, *Phys. Rev. E* **60**, 6421 (1999); R. Wackerbauer, *ibid.* **59**, 2872 (1999); A. Mielke, *Phys. Rev. Lett.* **84**, 818 (2000); B. Spagnolo, A. A. Dubkov, and N. V. Agudov, *Acta Phys. Pol. B* **35**, 1419 (2004).
- [3] N. V. Agudov and B. Spagnolo, *Phys. Rev. E* **64**, 035102(R) (2001); A. Fiasconaro, D. Valenti, and B. Spagnolo, *Physica A* **325**, 136 (2003); A. A. Dubkov, N. V. Agudov, and B. Spagnolo, *Phys. Rev. E* **69**, 061103 (2004); A. Fiasconaro, B. Spagnolo, and S. Boccaletti, *ibid.* **72**, 061110 (2005).
- [4] G. Parisi, *Nature (London)* **433**, 221 (2005); C. M. Dobson, *ibid.* **426**, 884 (2003); M. Acar, A. Becskei, and A. van Oudenaarden, *ibid.* **435**, 228 (2005); C. Lee *et al.*, *Nat. Rev. Mol. Cell Biol.* **5**, 7 (2004).
- [5] A. L. Pankratov and B. Spagnolo, *Phys. Rev. Lett.* **93**, 177001 (2004); H. Larralde and F. Leyvraz, *ibid.* **94**, 160201 (2005); E. V. Pankratova, A. V. Polovinkin, and B. Spagnolo, *Phys. Lett. A* **344**, 43 (2005).
- [6] P. W. Anderson, K. J. Arrow, and D. Pines, *The Economy as an Evolving Complex System* (Addison Wesley, Longman, 1988); P. W. Anderson, K. J. Arrow, and D. Pines, *The Economy as an Evolving Complex System II* (Addison Wesley, Longman, 1997).
- [7] R. N. Mantegna and H. E. Stanley, *An Introduction to Econophysics: Correlations and Complexity in Finance* (Cambridge University Press, Cambridge, 2000).
- [8] J.-P. Bouchaud and M. Potters, *Theory of Financial Risks* (Cambridge University Press, Cambridge, 2000).
- [9] R. Cont, *Quant. Finance* **1**, 223 (2001).
- [10] L. Bachelier, *Ann. Sci. Ec. Normale Super.* **III-17**, 21 (1900).
- [11] M. M. Dacorogna, R. Gencay, U. A. Müller, R. B. Olsen, and O. V. Pictet, *An Introduction to High-Frequency Finance* (Academic Press, New York, 2001).
- [12] S. L. Heston, *Rev. Financ. Stud.* **6**, 327 (1993).
- [13] J. Cox, J. Ingersoll, and S. Ross, *Econometrica* **53**, 385 (1985); J. P. Fouque, G. Papanicolau, and K. R. Sircar, *Derivatives in Financial Markets with Stochastic Volatility* (Cambridge University Press, Cambridge, 2000).
- [14] W. Feller, *Ann. Math.* **54**, 173 (1951).
- [15] A. Christian Silva, Richard E. Prange, and Victor M. Yakovenko, *Physica A* **344**, 227 (2004); A. Christian Silva, arXiv: physics/0507022 (unpublished).
- [16] G. Bonanno and B. Spagnolo, *Fluct. Noise Lett.* **5**, L325 (2005); *Mod. Probl. Stat. Phys.* **4**, 122 (2005).
- [17] S. Miccichè, G. Bonanno, F. Lillo, and R. N. Mantegna, *Physica A* **314**, 756 (2002).
- [18] A. A. Dragulescu and V. M. Yakovenko, *Quant. Finance* **2**, 443 (2002).
- [19] Y. Louzoun. and S. Solomon, *Physica A* **302**, 220 (2001); S. Solomon and P. Richmond, *Eur. Phys. J. B* **27**, 257 (2002); O. Malcai, O. Biham, P. Richmond, and S. Solomon, *Phys. Rev. E* **66**, 031102 (2002).
- [20] L. Borland, *Phys. Rev. E* **57**, 6634 (1998); *Quant. Finance* **2**, 415 (2002).
- [21] L. Borland, *Phys. Rev. Lett.* **89**, 098701 (2002).
- [22] P. Neu and R. Kühn, *Physica A* **342**, 639 (2004); J. P. L. Hatchett and R. Kühn, *J. Phys. A* **39**, 2231 (2006).
- [23] J.-P. Bouchaud and R. Cont, *Eur. Phys. J. B* **6**, 543 (1998).
- [24] J.-P. Bouchaud, *Quant. Finance* **1**, 105 (2001).
- [25] J.-P. Bouchaud, *Physica A* **313**, 238 (2002).
- [26] D. Sornette, *Phys. Rep.* **378**, 1 (2003).
- [27] B. M. Friedman, D. I. Laibson, and H. P. Minsky, *Brookings Papers on Economic Activity* **1989**(2), 137 (1989).
- [28] J. Masoliver, M. Montero, and J. Perelló, *Phys. Rev. E* **71**, 056130 (2005).
- [29] M. Montero, J. Perelló, J. Masoliver, F. Lillo, S. Miccichè, and R. N. Mantegna, *Phys. Rev. E* **72**, 056101 (2005).
- [30] E. Scalas, R. Gorenflo, and F. Mainardi, *Physica A* **284**, 376 (2000); F. Mainardi, M. Raberto, R. Gorenflo, and E. Scalas, *ibid.* **287**, 468 (2000); M. Raberto, E. Scalas, and F. Mainardi, *Physica A* **314**, 749 (2002); E. Scalas, cond-mat/0501261 (unpublished).
- [31] C. W. Gardiner, *Handbook of Stochastic Methods* (Springer, Berlin, 2004).
- [32] P. Hänggi, P. Talkner, and M. Borkovec, *Rev. Mod. Phys.* **62**, 251 (1990); E. Pollak and P. Talkner, *Chaos* **15**, 026116 (2005).
- [33] G. Bonanno, G. Caldarelli, F. Lillo, and Rosario N. Mantegna, *Phys. Rev. E* **68**, 046130 (2003).
- [34] G. Bonanno, G. Caldarelli, F. Lillo, S. Miccichè, N. Vandewalle, and R. N. Mantegna, *Eur. Phys. J. B* **38**, 363 (2004).